Experiments and mathematical models of black liquor gasification – influence of minor gas components on temperature, gas composition, and fixed carbon conversion

PER CARLSSON, MAGNUS MARKLUND, ERIK FURUSJÖ, HENRIK WIINIKKA, and RIKARD GEBART

ABSTRACT: In this work, predictions from a reacting Computational Fluid Dynamics (CFD) model of a gasification reactor are compared to experimentally obtained data from an industrial pressurized black liquor gasification plant. The data consists of gas samples taken from the hot part of the gasification reactor using a water cooled sampling probe. During the considered experimental campaign, the oxygen-to-black liquor equivalence ratio (λ) was varied in three increments, which resulted in a change in reactor temperature and gas composition. The presented numerical study consists of CFD and thermodynamic equilibrium calculations in the considered λ-range using boundary conditions obtained from the experimental campaign. Specifically, the influence of methane concentration on the gas composition is evaluated using both CFD and thermodynamic equilibrium. The results show that the main gas components (H_2, CO, CO_2) can be predicted within a relative error of 5% using CFD if the modeled release of H_2S and CH_4 are specified a priori. In addition, the calculations also show that the methane concentration has large influence on the reactor outlet temperature and final carbon conversion.

Application: This work shows how predictions from a CFD model compare to experimental data and thermodynamic equilibrium calculations. By comparing predictions from the mathematical models with experimental data and developing the models, a deeper understanding of a complex process can be achieved. If properly validated, the mathematical models can then be used in optimization and scale up of entrained flow gasifiers.

Black liquor gasification could potentially replace or complement the conventional recovery boiler used in the kraft pulp making process. Since 2005, the technology vendor Chemrec AB has operated a 3 MW development plant (DP-1) for pressurized entrained flow high temperature black liquor gasification (PEHT-BLG) [1] for a total accumulated operating time in excess of 12000 h. The gasification plant (see schematic layout in **Fig. 1**) was built in order to demonstrate that the technology is ready for scale up and to enable research and development of the technology. In a closely connected research program aimed at eliminating scientific obstacles for commercialization, experiments in the plant were carried out and process models were developed.

The parts of the DP-1 black liquor gasifier are mainly made up of (Fig. 1) a slagging refractory lined entrained-flow gasification reactor with a gas assisted burner nozzle producing small black liquor droplets that are directly gasified at about 1000°C to produce a "raw" syngas and a liquid smelt containing mainly Na_2CO_3 and Na_2S; a quench cooler beneath the reactor where the product gas and smelt are separated and the smelt is dissolved in water, forming green liquor; and a

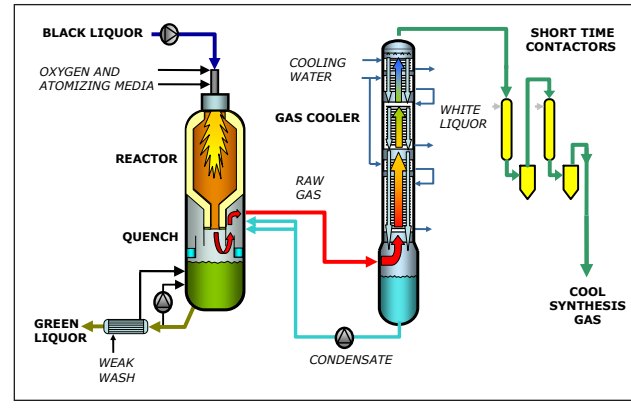

1. Schematic drawing of the PEHT-BLG process (courtesy of Chemrec AB).

counter current condenser that cools the syngas and condenses water vapor and other condensable species that may be present. In the current work, predictions from a Computational Fluid Dynamics (CFD) model of the gasification reactor part are compared to gas samples taken from inside of the hot reactor using a water cooled suction probe [2,3]. During the experiments, the oxygen-to-black liquor equivalence ratio

was varied in three increments affecting the temperature and gas composition inside the reactor.

The aim of the present work was to assess the performance of an updated version of a previously developed CFD reactor model [4] and to identify possible modifications to improve the model predictions. Special emphasis is put on the influence of methane concentration on local gas composition. Furthermore, to aid in the evaluation of the CFD model predictions, thermodynamic equilibrium calculations were performed using the commercially available thermodynamic equilibrium and phase diagram software FactSage [5] and an in-house thermodynamic equilibrium code developed by Furusjö (a co-author of this paper).

EXPERIMENTAL

Gas samples were withdrawn from the hot part of the DP-1 gasification reactor using a water-cooled gas sampling probe specially designed to quench the gas and, thereby, to freeze any possible chemical reactions when the gas flows through the probe [2]. The gas samples were collected approximately 0.6 m above the outlet of the DP-1 gasification reactor (see position in **Fig. 2**).

The collected gas samples were analyzed with respect to CH_4, CO, CO_2, H_2, N_2, H_2S, COS, and O_2/Ar using a Varian CP-3800 gas chromatograph. During the experimental campaign, which took place in October of 2008, several operating

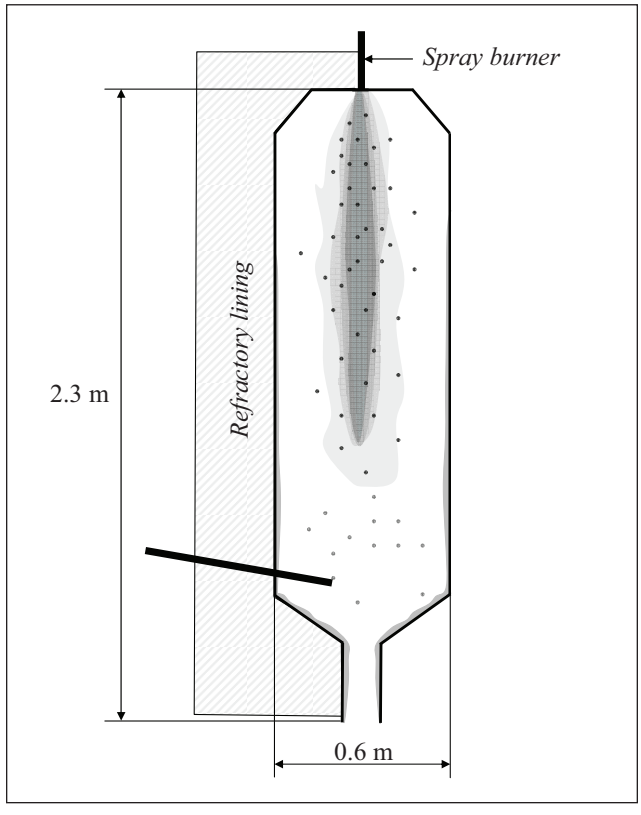

2. Sketch of the DP-1 gasification reactor with the size and position of the gas sampling probe indicated. Gas samples were collected at the tip of the gas sampling probe.

Variable	Unit	Case		
		-	0	+
Pressure	bar(g)	27	27	27
Black liquor mass flow rate	kg/h	870	870	870
Black liquor pre-heat temperature	°C	140	140	140
O_2 mass flow rate	kg/h	235	254	265
N_2 mass flow rate	kg/h	47	47	47
O_2 / BL	-	0.270	0.292	0.305
λ	-	0.403	0.435	0.454

I. Operating parameters for the DP-1 gasifier during the experimental campaign.

parameters were varied [3] and in the present work the obtained results from the variations in oxygen-to-black liquor equivalence ratio (defined as $\lambda=(x_{O2}/x_{fuel})/(x_{O2,stoich}/x_{fuel,stoich})$, where x is mol fraction) were used to evaluate the performance of the CFD reactor model. The experimental data consist of gas compositions for three different equivalence ratios. **Table I** summarizes the main operational parameters in the experiments.

As Table I shows, only the oxygen mass flow rate was used to get a corresponding change in oxygen to black liquor mass flow rate ratio and consequently to the oxygen-to-black liquor equivalence ratio during the experimental campaign. The experimentally obtained results are described and evaluated in Carlsson et al. [3] but are reproduced here in **Fig. 3** for the sake of clarity.

MATHEMATICAL MODELING

In the current work, CFD was used as a tool to predict gas composition and temperature distribution inside the DP-1 gasification reactor. To further aid in the evaluation of the results, additional thermodynamic equilibrium calculations were performed. The following subsections contain general descriptions of the CFD model and the thermodynamic equilibrium code, as well as the implemented boundary conditions used to predict the influence of λ on the local gas composition.

CFD model

The DP-1 reactor is an axi-symmetric entrained-flow reactor with the spray burner centrally placed at the reactor top (Fig. 1). The reactor internal dimensions are 2.3 m in height and 0.6 m in inner diameter. Based on the rotational symmetry, the reactor geometry was modeled as a 2D slice using periodic azimutal boundary conditions. Regarding the wall boundary, estimates have shown that the heat loss in the plant through the reactor wall is approximately 90 kW or about 3% of the total thermal throughput at full capacity. Based on this, heat losses through the modeled refractory lined reactor wall were specified using a uniformly distrib-

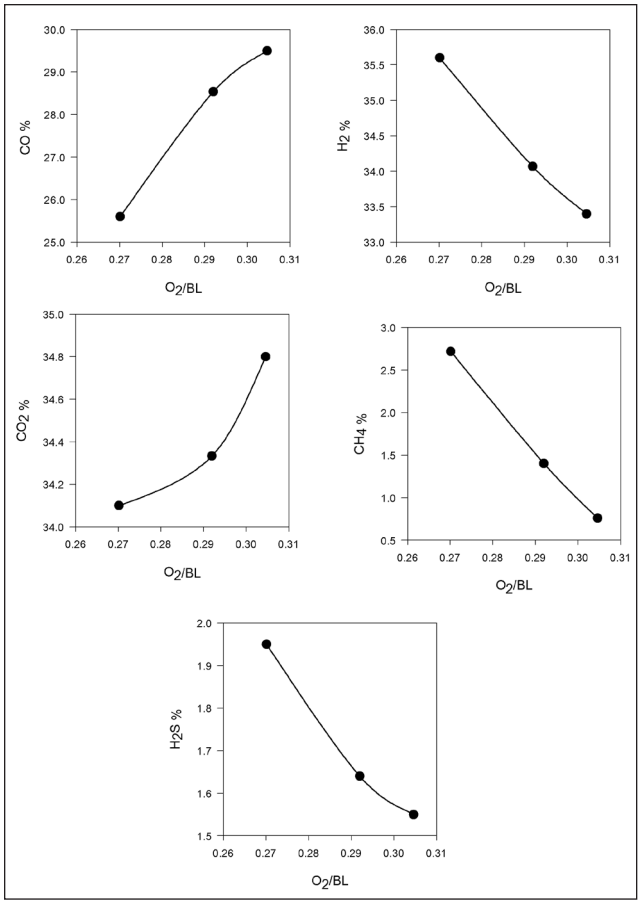

3. Experimentally obtained results taken from Carlsson et al. [3].

uted heat loss along the wall.

The burner was modeled as a simplified spray burner with concentrical annular inlets where oxygen and discrete black liquor droplets enter the gasifier at a prescribed range of angles and velocities. The two-phase flow consisting of dispersed black liquor particles and gases was modeled using the Euler – Lagrange formulation [6]. In the present paper, the black liquor spray was represented by 1003 discrete particles having a fitted Rosin Rammler distribution of power 2 and size 200 μm. The droplet size distribution and flow velocity are consistent with data from nozzle experiments measured by phase Doppler anemometry [7].

To model turbulence, the k-ε model with scalable wall functions [8] was used. To include effects of turbulence on the discrete particles, a turbulent dispersion model was introduced as suggested by Gosman and Ioannides [9].The radiative heat transfer was modeled using the Discrete Transfer radiation model by Lockwood and Shah [10], treating the wall as optically smooth with a radiative emissivity of 0.5. The absorption coefficient for the gas was calculated as the mass weight average of the participating species.

In the present paper, the simplified gas phase reaction scheme by Jones and Lindstedt [11], as concerns Reactions (1-3) and (5), together with CO oxidation (Reaction (4)) [12] was implemented as done by others [13,14,15].

$$CH_4 + \tfrac{1}{2}O_2 \rightarrow CO + 2H_2 \quad (1)$$

$$CH_4 + H_2O \rightarrow CO + 3H_2 \quad (2)$$

$$H_2 + \tfrac{1}{2}O_2 \rightarrow H_2O \quad (3)$$

$$CO + \tfrac{1}{2}O_2 \rightarrow CO_2 \quad (4)$$

$$CO + H_2O \rightarrow CO_2 + H_2 \quad (5)$$

To include turbulent mixing effects on reaction rates, the Eddy Dissipation Model (EDM) [19] was used together with Finite Rate Chemistry (FRC). The EDM-FRC model calculates the turbulent mixing rate and kinetic reaction rate and uses the minimum (i.e., slowest) of the two. Note that Reactions (1,3,4) above were modeled using pure EDM, assuming that the reaction rates are controlled by turbulent mixing only, and Reaction (2) was modeled using the combined EDM/FRC model, assuming that the reaction is controlled by mixing close to the burner and kinetically controlled in the downstream region (lower part of the reactor). Furthermore, Reaction (5) was modeled using only the FRC model, thus ensuring that the reaction evolves towards equilibrium [20]. Regarding the sulfur chemistry in the gas phase, H_2S (released during pyrolysis) was treated as inert.

Char gasification and smelt formation reactions were modeled as Reactions (6-8) below belusing the reaction mechanisms and coefficients as described by Marklund [4].

$$C + H_2O \rightarrow CO + H_2 \quad (6)$$

$$C + CO_2 \rightarrow 2CO \quad (7)$$

$$C + \tfrac{1}{2}Na_2SO_4 \rightarrow \tfrac{1}{2}Na_2S + CO_2 \quad (8)$$

The model was implemented in the commercial CFD software package Ansys CFX where drying and pyrolysis were treated in a similar manner as char gasification and smelt formation through multiphase reactions implemented in user defined FORTRAN subroutines.

Material description

In the CFD model, the materials have to be described as specified species. Hence, the elemental or ultimate analysis needed to be transformed into the considered species. Based on the detailed elemental composition in Table II, the ultimate analysis was simplified by lumping K together with Na and neglecting the small amounts of Cl and N, thus forming a simplified elemental composition of the modeled black liquor (**Table II**).

By converting from mass to mole fractions, the simplified ultimate analysis was written as a row vector (**ev**) where **ev**(*j*) is the molar fraction of element *j*. The different species were then described by a matrix **S**, defined as follows in Eq. (1):

Ultimate Analysis (dry solids)		Relative Uncertainty	CFD Pre-model Inputs
	%wt	%	%wt
C	31.3	2.0	31.3
H	3.4	6.0	3.4
O*	37.2	9.1**	37.3
N	0.1	20.0	0.0
S	5.6	13.0	5.6
Na	20.1	8.0	22.4
K	2.3	8.0	0.0
Cl	0.1	13.0	0.0
Proximate Analysis			
Moisture	24.8	2.0%	
Volatiles	N/A		
Fixed carbon	N/A		
Ash	N/A		
HHV MJ/kg	12.57	1.6%	

by difference,by difference from uncertainties in participating elements using extremes*

II. Proximate and ultimate analysis for black liquor used in the experimental campaign and the simplified description used as input to the CFD model.

$$\mathbf{S} = \begin{bmatrix} S_{ij} & \cdot & \cdot \\ \cdot & \cdot & \cdot \\ \cdot & \cdot & S_{m} \end{bmatrix} \qquad i \rightarrow 1:m \tag{1}$$

Where m is the number of considered species that should be present in the CFD-model and n is the number of elements in the element vector. The matrix elements ($\mathbf{S}_{ij}$) describe how many moles of element j it takes to construct one mol of specie $\mathbf{S}_i$. From the species matrix ($\mathbf{S}$) and the element vector ($\mathbf{e}_v$), a system of linear equations (Eq. (2)) was formulated:

$$\mathbf{S}^T \cdot \mathbf{p} = \mathbf{e}_v{}^T \tag{2}$$

Where $\mathbf{p}(i)$ is the mol fraction for each respective specie. Since the number of model species was greater than the number of elements, the system is underdetermined; that is, the number of unknowns ($\mathbf{p}$) was greater than the number of formulated equations ($\sim\mathbf{e}_v$). To resolve this, a constraint matrix ($\mathbf{C}$) and a constraint vector ($\mathbf{c}_v$) were defined and a similar system as in Eq. (1) was formulated. The matrix elements of $\mathbf{C}$ and the constraint vector ($\mathbf{c}_v$) were used to define ratios between the different species, as in Eq. (3):

Case	O_2 / BL	Sulfur to gas phase (molar of total)	CH_4 as inert (molar of total)
-	0.270	40.0%	25.4%
0	0.292	33.5%	12.4%
+	0.305	31.5%	6.7%

III. Constraints on sulfur and CH_4 release during pyrolysis in the CFD calculations.

$$\mathbf{C} = \begin{bmatrix} C_{il} & \cdot & \cdot \\ \cdot & \cdot & \cdot \\ \cdot & \cdot & C_{mm} \end{bmatrix} \quad l \rightarrow 1:m, \quad \mathbf{c}_v = (c_{v,i}, \cdot, \cdot, c_{v,m}), \quad \mathbf{C} \cdot \mathbf{p} = \mathbf{c}_v \tag{3}$$

In order to solve the system of equations and obtain the composition of the different species in the black liquor, the following constraints were used (as in [4]):

- Half of the carbon was modeled as fixed, i.e., char.
- The molar ratio between CO and CO_2 was equal to unity in the pyrolysis step.
- The molar ratio Na_2SO_4 over Na_2S was 8.
- The molar concentration of NaOH in dry black liquor was specified to 0.50%.
- All water is evaporated during drying.

Currently, the CFD-model does not contain a detailed reaction mechanism for H_2S. Thus, the amount of H_2S released during pyrolysis will not react in the gas phase or with the smelt in the black liquor particles. However, as can be seen in Fig. 3, the H_2S concentration varies with the oxygen-to-black liquor mass flow rate ratio. To take this into consideration, different amounts of H_2S were released during pyrolysis as a function of the oxygen-to-black liquor equivalence ratio. Furthermore, previous calculations [4] have shown that the CFD model is unable to predict the CH_4 concentration at the outlet of the gasifier. To investigate the influence of this, part of the CH_4 released during pyrolysis was modeled as inert in a similar manner as with H_2S. **Table III** summarizes the constraints on H_2S and CH_4.

The linear system of equations described by Eq. (2) was solved using the least squares method under the constraints described previously.

$$\begin{cases} \boldsymbol{A} = \boldsymbol{S} \cdot \boldsymbol{S}^T \\ \boldsymbol{b} = \boldsymbol{S} \cdot \boldsymbol{e}_v{}^T \end{cases} \Rightarrow \boldsymbol{A} \cdot \boldsymbol{p} = \boldsymbol{b}, \quad \min_p \left\| \boldsymbol{A} \cdot \boldsymbol{p} - \boldsymbol{b} \right\|_2^2 \quad \textit{subject to the constraints} \quad \begin{cases} \boldsymbol{C} \cdot \boldsymbol{p} = \boldsymbol{c}_v \\ 0 \le \boldsymbol{p} \le 1 \end{cases} \tag{4}$$

Table IV presents the material composition obtained from this solution method. As can be seen in this table, there

CFD Proximate Analysis		Case		
		-	0	+
	Specie	% wt	% wt	% wt
Moisture	**H_2O(l)**	**24.8**	**24.8**	**24.8**
Volatiles	H_2S(g)	1.8	1.5	1.4
	CO(g)	5.9	5.9	5.8
	CO_2(g)	9.3	9.2	9.2
	H_2(g)	1.2	1.2	1.2
	CH_4(g)Inert / CH_4(g)Total	1.18/ 4.65	0.60/ 4.83	0.33/ 4.89
Fixed carbon	**C(s)**	**11.8**	**11.8**	**11.8**
Ash	Na_2SO_4(l)	10.0	11.0	11.3
	Na_2S(l)	0.7	0.8	0.8
	Na_2CO_3(l)	28.5	27.6	27.4
	NaOH(l)	1.4	1.4	1.4
HHV MJ/kg		**12.62**	**12.60**	**12.60**

IV. Proximate analysis for black liquor used in the CFD calculations.

is a small difference in the experimentally obtained heating value (Table II) and the modeled heating values. To ensure consistency between the experimental results and the model, pyrolysis was treated as a multiphase reaction, with the heat of reaction chosen so that the modeled and experimental heating value became equal.

Thermodynamic equilibrium model

The thermodynamic equilibrium simulations used in this paper were carried out using FactSage [5] and SIMGAS, which is an in-house gasification simulation tool. Details regarding FactSage are covered extensively in the literature and will not be explained here.

SIMGAS is implemented in the Matlab platform and based on system Gibbs energy minimization under the assumption of ideal mixtures. The tool uses an active-set method [16] to solve the constrained non-linear minimization problem with the chemical composition of gas and smelt phases as independent variables. To obtain a good starting point for the non-linear optimization loop, an approximate linear problem is solved at first. The element balances are implemented as linear constraints.

The approach uses a set of chemical components that are postulated to be present in the equilibrium mixture. The quantitative composition of the mixture is then calculated by the minimization algorithm, based on thermodynamic data of the components and element balances. This may result in a mixture composition where some of the postulated components are not present; i.e., the calculated concentration is zero but the algorithm cannot "suggest" new components, so it is of utmost importance to specify a relevant component list. The components listed in **Table V** were used based on experience from pilot plant operations and simulations using other larger sets of chemical components. The thermodynamic data were taken from Lindberg [17], disregarding the interaction parameters because the thermodynamic model does not include interactions.

Gas	Smelt
CO	Na_2CO_3
H_2	Na_2S
CO_2	NaOH
H_2O	NaCl
H_2S	Na_2SO_4
COS	K_2CO_3
N_2	K_2S
CH_4	KOH
	KCl
	K_2SO_4
	C(s)

V. Components used in the thermodynamic model of the system.

The reactor energy balance is solved in an outer loop for oxygen supply or equilibrium temperature (heat losses are accounted for). This numerical problem is considerably simpler and is solved by a safe-guarded secant method [18]. The thermodynamic equilibrium model includes functionality to use user-specified concentrations for some components, primarily methane and hydrogen sulfide. The resulting gas and smelt composition calculated when this possibility is used is an equilibrium composition, given the fixed or empirically calculated concentrations.

Boundary conditions and constraints

The numerical study consists of six CFD calculations, three thermodynamic equilibrium calculations using FactSage, and three using SIMGAS. The boundary conditions for all the calculations were taken as the measured values obtained from the DP-1 process monitoring system during the experimental campaign. Notice that in the CFD model, H_2S is not part of the reaction scheme (Reactions (1-8)); instead, it is treated as an inert and specified in the material description (Table IV). A similar simplification is made for Na_2CO_3 and NaOH. Currently, the CFD model predictions for CH_4 concentration are far below the measured values, presumably as a result of an improper description of the reaction kinetics. To investigate the influence of methane concentration on gas composition and temperature, part of the CH_4 was treated as inert in three of the CFD calculations (Tables III and IV).

Thermodynamic equilibrium calculations were performed in order to determine the gas composition if all reactions (gas and particle phase) would proceed all the way to equilibrium and used for comparison with the CFD results. As a reference, equilibrium calculations using FactSage were performed at the predicted outlet temperature obtained from CFD. The inlet composition was specified according to Table

Case	Method	Temperature	Constrained H_2S	Constrained CH_4
- 0 +	Thermodynamic equilibrium FactSage	CFD outlet tempearture	No	No
- 0 +	Thermodynamic equilibrium SIMGAS	Energy equation	Yes	Yes
- 0 +	CFD	Energy equation	Yes	Yes
- 0 +	CFD	Energy equation	Yes	No

VI. Numerical method and case description; boundary conditions not specified are according to Table I and Table II.

II, i.e., as received from analysis, including the moisture. Oxygen and nitrogen fractions were set to match the oxygen-to-black liquor mass flow rate ratio. In FactSage, there is no easy way to set the wall heat loss or to solve the energy equation; hence, the calculations were performed at the temperature obtained from the CFD calculations. However, in SIMGAS, the energy balance is solved together with gas composition iteratively. To get a comparison between the equilibrium code and the CFD model, the CH_4 and H_2S concentrations were specified according to the experimentally obtained values in a similar manner as in the CFD calculations. **Table VI** summarizes the performed calculation.

RESULTS

Figure 4 shows the typical temperature distribution obtained from the CFD model. Notice that in the high oxygen-to-black liquor equivalence ratio case, the high temperature region stretches further down in the reactor and is significantly wider. In the rest of the reactor, the temperature is relatively uniform, particularly in the lower parts close to where the experimental samples were collected.

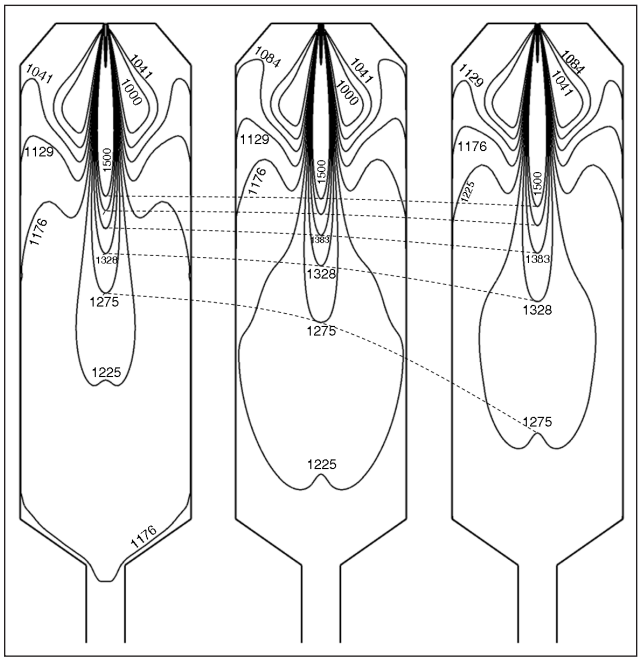

4. Temperature distribution obtained from the CFD calculations. From left to right: λ = 0.40, 0.44, and 0.45. The dotted lines indicate where the temperature contours coincide along the center axis for the different cases.

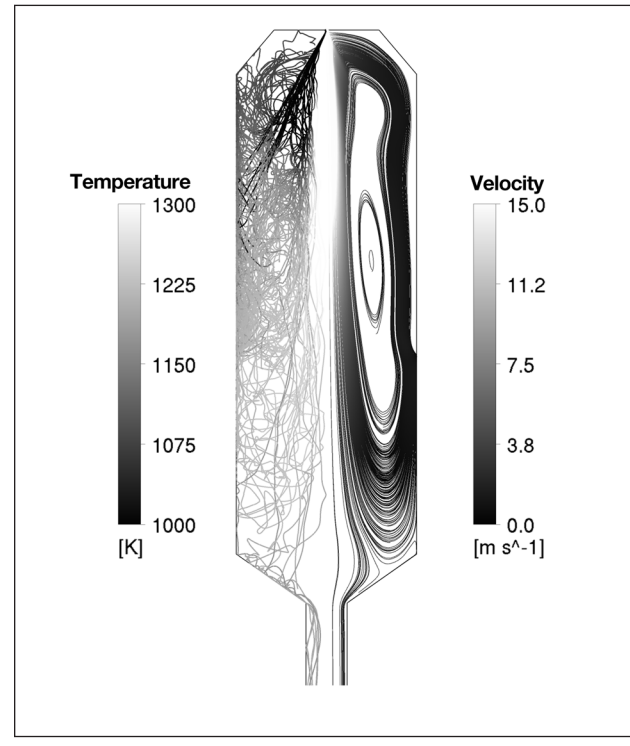

5. Part of the particle trajectories colored by temperature (left). Streamlines colored by velocity (right).

The cold regions in the upper part of the reactor can be explained by the heat absorbed by the droplets in the drying step implemented in the CFD model (**Fig. 5**). The right part of Fig. 5 also shows the large recirculation zone that is characteristic for this type of gasifier. In **Fig. 6**, the dry and nitrogen free molar fractions of CH_4 and H_2S (minor gas components) are presented as a function of oxygen-to-wet black liquor mass flow rate ratio (Table I). The methane concentration was prescribed as described previously in one set of the CFD calculations and in one set of the thermodynamic equi-

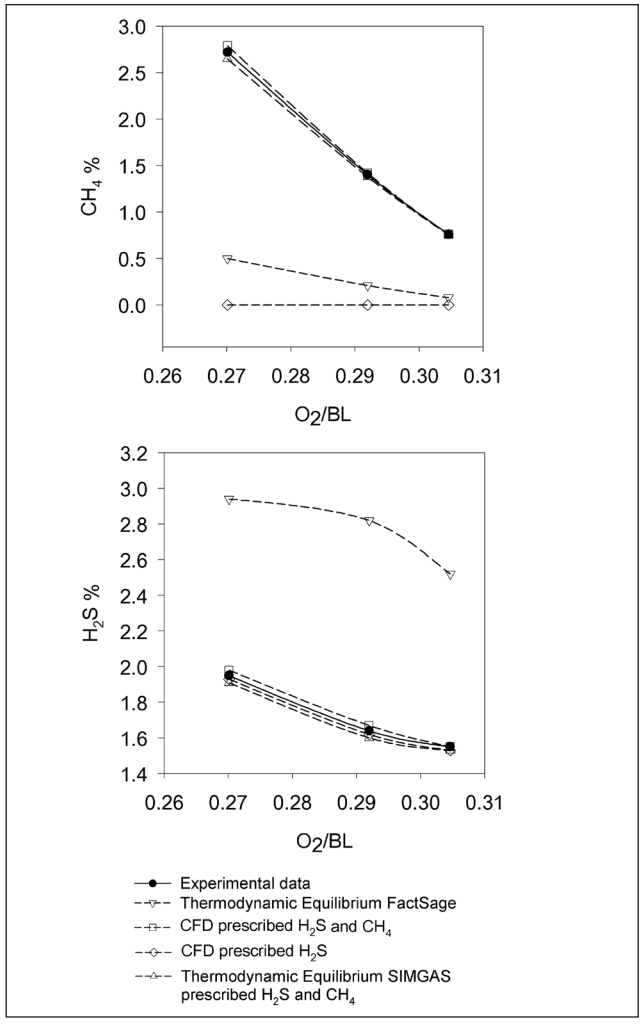

6. Molar concentration for the minor gas components obtained from experiments and FactSage predictions, and as specified in the CFD and SIMGAS thermodynamic equilibrium calculations.

librium calculations (Table III). The thermodynamic equilibrium calculations performed with FactSage show a clear divergence from the experimental results, as do the CFD calculations with no restrictions on methane.

Figure 7 presents the dry and nitrogen free molar fraction of the main gas components (CO, CO_2, and H_2). The general trends (decreasing/increasing concentration) are predicted by both the CFD model and the two equilibrium models, at least for the two points with higher oxygen-to-black liquor mass flow rate ratio. At the lower oxygen-to-black liquor ratio, the solution obtained with FactSage with no constraints on CH_4 or H_2S deviates from the trend and predicts approximately the same CO level as obtained at the middle oxygen-to-black liquor ratio. The values obtained by the CFD model (gas composition) are taken as field values from the calculated position of the sampling probe tip.

The left graph of **Fig. 8** shows the reactor outlet temperature obtained from the in-house thermodynamic equilibrium code and the CFD calculations. The right graph in Fig. 8 shows the fixed carbon conversion for the two CFD models. Notice that there is a significant difference in fixed carbon conversion. When CH_4 is included as an inert, the fixed carbon conversion increases approximately 8% (relative) for the lowest oxygen-to-black liquor mass flow rate ratio. Both thermodynamic equilibrium codes predict 100% fixed carbon conversion and are not shown.

There are only small variations in the smelt composition (**Table VII**) for the main species (Na_2, CO_3, and Na_2S approximately ±3 % units on mass basis) when varying λ and assuming thermodynamic equilibrium with constraints on CH_4 and H_2S. Furthermore, the smelt composition obtained using thermodynamic equilibrium is in good agreement with the one obtained from the CFD model using the least squares method on the simplified material description described previously.

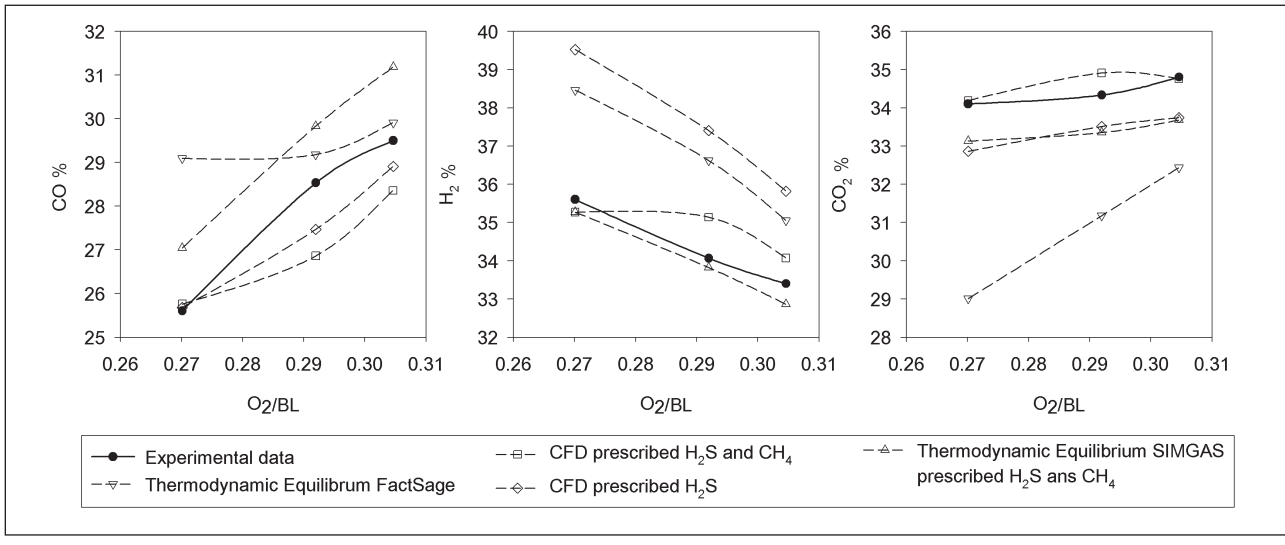

7. Molar concentration for the main gas components: obtained from experiments, predicted using CFD, and calculated assuming thermodynamic equilibrium with specified CH_4 and H_2S concentration.

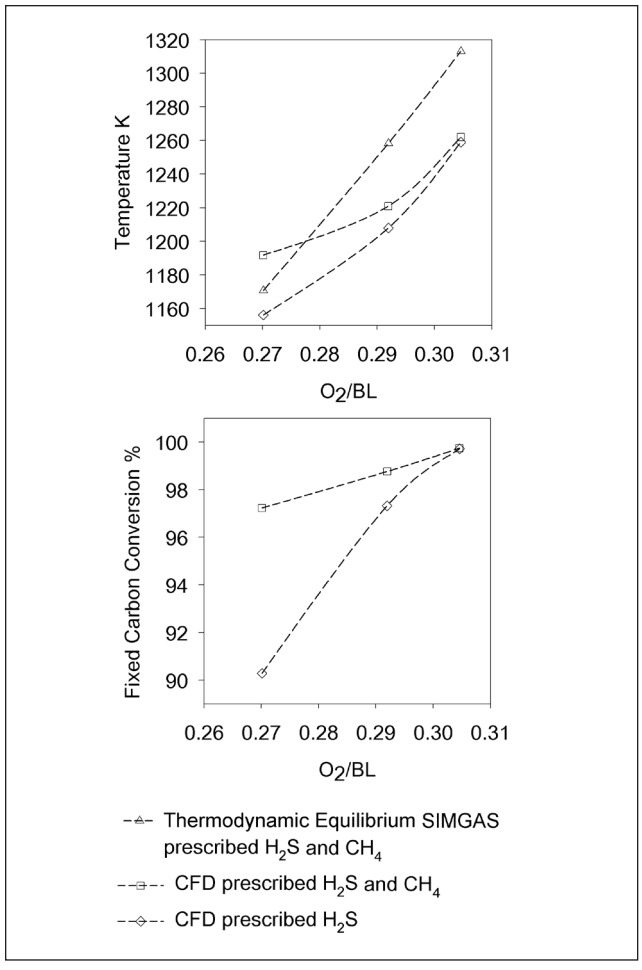

8. Reactor outlet temperature obtained from the in-house thermodynamic equilibrium code and from the CFD calculations (top) and fixed carbon conversion using the two CFD models (bottom).

DISCUSSION

When part of CH_4 is included as inert in the calculation, the predictions show much better agreement with the experimentally obtained values compared to the case where no inert CH_4 is considered. This is valid for both the equilibrium and CFD calculations. If CH_4 and H_2S are not specified but calculated using thermodynamic equilibrium, CH_4 concentration in the dry, nitrogen free gas is ~0.2% and H_2S is ~2.8 % for λ = 0.44. This also has an effect on the major gas components, with the most predominant difference at the low temperature case (λ = 0.40). The major gas components, when predicated by CFD, are close to equilibrium (within 5% by comparing with the equilibrium constant). Hence, given the good agreement with the experimental data (relative error less than 5%) it could be argued that the major gas components are at or close to equilibrium and the main mechanism is the water gas CO shift reaction. Furthermore, H_2S and CH_4 are not at thermodynamic equilibrium (cannot be predicted by a thermodynamic equilibrium code) and the dominating mechanisms are not adequately described in the CFD model. Given that the CFD predictions show good agreement (when H_2S and CH_4 concentrations are prescribed) with the experimentally obtained results, it is possible that the flow field is also adequately predicted. However, this remains to be verified by further experiments.

There is a significant difference in fixed carbon conversion between the performed CFD calculations (Fig. 8). This is particularly true for the low lambda (i.e., low temperature) case when all of the available CH_4 is allowed to react, and the fixed carbon conversion is as low as 90.3%. This should be compared to 97.2% for the case when CH_4 concentration in the gas is constrained. For the high temperature (i.e., high lambda) case, the fixed carbon conversion is 99.7% for both the CFD model descriptions. In the high temperature case, the temperatures are also very similar between the two CFD models, which could explain the similarities in fixed carbon conversion. It is worth mentioning that, during normal operation of the gasifier, the fixed carbon conversion is very close to 100% because no char or soot is detected in the green liquor or the green liquor dregs.

Figure 4 shows the temperature distribution obtained using CFD. The spreading of the hot region (flame region) increases significantly when lambda is increased. It is possible that the hot region is even longer in the real reactor, given the deficiencies in the k-ε turbulence model, where the spreading rate is over predicted for round jets [21]. In the lower part of the reactor, the temperature appears to be rather uniform, which, from an experimental point of view, is encouraging. The lack of temperature gradient would support that the gas composition at the sample point is similar to the one obtained at the outlet [3].

The methane concentration has a significant influence on the gas temperature. If all methane is allowed to react, the reactor outlet temperature is lower compared to when methane is constrained. This becomes apparent for the low oxygen-to-black liquor equivalence ratio case when there is no constraint on methane. The carbon conversion is about 90%, which effectively means that less energy is spent on converting fixed carbon to gas through the gasification reactions. Consequently, if less energy is spent on converting fixed carbon to gas, the gas temperature should be higher. However, this is not observed. The explanation for this is the endothermic steam methane reforming reaction (Reaction 2). Thus, methane that is not oxidized close to the flame will consume energy as it converts to CO and H_2. The conversion of methane will reduce the gas temperature, resulting in reduced reaction rates for the gasification reactions with poor fixed carbon conversion as a result. For the highest oxygen-to-black liquor equivalence ratio, the methane concentrations are about three times less than for the low ratio, and the influence from methane concentrations is significantly reduced.

CONCLUSIONS AND FUTURE WORK

From the calculations performed in this work, it is clear that the methane concentration and the conversion of methane have a significant effect on the major gas components. The

Case		-		0		+	
Component %wt	Method	CFD	SIMGAS	CFD	SIMGAS	CFD	SIMGAS
Na_2CO_3		78.2	73.0	76.7	69.5	76.3	68.9
Na_2S		17.0	17.1	18.9	19.7	19.6	19.9
NaOH		3.9	1.6	3.9	2.3	4.0	2.9
NaCl		-	0.1	-	0.1	-	0.1
Na_2SO_4		0.0	0.0	0.0	0.0	0.0	0.0
K_2CO3		-	6.6	-	6.8	-	5.7
K_2S		-	0.6	-	0.0	-	0.7
KOH		-	0.7	-	1.2	-	1.4
KCl		-	0.3	-	0.3	-	0.3
K_2SO_4		-	0.0	-	0.0	-	0.0
C(s)		0.9	0.0	0.4	0.0	0.1	0.0
$\Sigma\ CO_3^{2-}$		78.2	79.6	76.7	76.3	76.3	74.6
$\Sigma\ S^{2-}$		17.0	17.7	18.9	19.7	19.6	20.7
$\Sigma\ OH^-$		3.9	2.3	3.9	3.4	4.0	4.4
$\Sigma\ SO_4^{2-}$		0.0	0.0	0.0	0.0	0.0	0.0
$\Sigma\ Cl^-$		-	0.4	-	0.4	-	0.4

VII. Smelt composition at the outlet of the reactor calculated with SIMGAS and CFD with prescribed H2S and CH4 levels.

methane concentration affects gas temperature because of the endothermic steam methane reforming reaction. In addition, the steam methane reforming reaction contributes to a displacement of the major gas components, because one mole of methane reacting with water vapor will result in three moles of H_2 and one mole of CO. In summarizing this work, the following conclusions can be drawn:

- The main gas components can be predicted both with the present CFD model and thermodynamic equilibrium if CH_4 and H_2S concentrations are prescribed.
- The CH_4 concentration in the gas has a significant influence on the main gas components (H_2, CO, CO_2).
- The fixed carbon conversion increases when part of the methane is treated as inert.
- CH_4 and H_2S are not in equilibrium in the DP-1 black liquor gasifier.
- The main gas components are close to equilibrium at the outlet of the DP-1 black liquor gasifier.

In the future work, the focus should be on implementation of a more detailed mechanism for the formation and conversion of H_2S and CH_4 in the CFD code. **TJ**

EDITOR'S NOTE

This paper was presented at the 2010 International Chemical Recovery Conference (ICRC) in Williamsburg, VA, where it received a Best Paper Award.

ACKNOWLEDGMENTS

The authors of this paper would like to thank the Swedish Energy Agency, Mistra, Smurfit Kappa Kraftliner AB, SCA Packaging AB, Södra Cell AB, Sveaskog AB, Chemrec AB, and the County Administrative Board of Norrbotten for funding this work through the BLG II research program.

LITERATURE CITED

1. Lindblom, M. and Landälv, I., *TAPPI Eng., Pulping Environ. Conf.*, TAPPI Press, Atlanta, 2006, Conf. CD.
2. Wiinikka, H., Carlsson, P., Granberg, F., et al., *Fuel* 89(9): 2583(2010).
3. Carlsson, P., Wiinikka, H., Marklund, M., et al. *Fuel* 89(12): 4025(2010).
4. Marklund, M., Tegman, R., and Gebart, R., *IFRF Combust. J.*, Article No. 200801.
5. Bale, C.W., Belisle, E., Chartrand, P., et al., *CALPHAD* 33(2):295(2009)
6. Crowe, C., Sommerfeld, M. and Tsuji, Y., *Multiphase Flows with Droplets and Particles*, CRC Press LLC, Boca Raton, FL, 1998.
7. Marklund, M., "Pressurized entrained-flow high temperature black liquor gasification," Ph.D. thesis, Luleå University of Technology, Luleå, Sweden, 2006.
8. Wilcox, D.C., *Turbulence Modeling for CFD*, Griffin Printing, Glendale, CA, 1993.
9. Gosman, A.D. and Ioannides, E., *AIAA J.* 81: 0323(1981).
10. Lockwood, F.C. and Shah, N.G., *Proc. Combust. Inst.* 18: 1405(1981).
11. Jones, W.P. and Lindstedt, R.P., *Combust. Flame* 73: 233(1988).

12. Westbrook, C.K. and Dryer, F.L., *Combust. Sci. Technol.* 27: 31(1981).

13. Fletcher, D.F., Haynes, B.S., Christo, F.C., et al., *Appl. Math. Modell.* 24: 165(1999).

14. Watanabe, H. and Otaka, M., *Fuel* 85: 1935(2006).

15. Yang W., Ponzio A., Lucas C, et al., *Fuel Process. Technol.* 87: 235(2005).

16. Mathworks Inc., *Matlab 2009b, Optimization Toolbox Documentation*, Natick, MA, 2009.

17. Lindberg, D., "Thermochemistry and melting properties of alkali salt mixtures in black liquor conversion processes," Ph.D. thesis, Åbo Akademi University, Åbo, Finland, 2007.

18. Dahlquist, G. and Björck, Å., *Numerical Methods in Scientific Computing*, Society for Industrial and Applied Mathematics, Philadelphia, 2008.

19. Magnussen, B.F. and Hjertager, B.H., *Proc. Combust. Inst.* 16: 719(1976).

20. Brink A., Mueller C., Kilpinen P., et al., *Combust. Flame* 123: 275(2000).

21. Pope, S.B., *Turbulent Flows*, Cambridge University Press, Cambridge, 2000.

ABOUT THE AUTHORS

High pressure, high temperature black liquor gasification can be a complement or a substitute to the conventional recovery boiler. The technology is just on the verge of being fully commercialized and scale-up operation is in progress. To aid with optimization and scale-up, reliable computational tools are of great importance.

In this work, two different types of computational models (CFD and thermodynamic equilibrium) have been used to predict the gas composition inside the gasification reactor. The predictions have then been compared to experimental data (obtained by our research group) and show very good agreement. Surprisingly, small concentrations of methane have a large influence on the temperature in the gasification reactor. Consequently, this will affect both the main gas components and the fixed carbon conversion.

The large differences in time and length scale between the convective flow (order of reactor dimensions) and the chemical reactions (order of flame thickness) makes modeling of gasification or combustion challenging. In this work, we were able to overcome the problem by careful selection of time steps for the momentum, continuity, and energy equations, respectively. In the future, the CFD model will be further refined so it can be used to accurately predict the behavior of entrained flow gasifiers of arbitrary size using different kinds of fuels.

Per Carlsson is research associate at the Energy Technology Centre in Piteå and graduate student at Luleå University of Technology, Magnus Marklund is senior scientist/group leader, Henrik Wiinikka is senior scientist/group leader, and Rikard Gebart is CEO with the Energy Technology Centre in Piteå and Associate Professor at Luleå University of Technology, Sweden. Erik Furusjö is process engineer with Chemrec AB in Stockholm Sweden. E-mail Carlsson at per.carlsson@etcpitea.se.

Carlsson

Marklund

Wiinikka

Gebart

Furusjö